Gynecologic Oncology 194 (2025) 60–70

Contents lists available at ScienceDirect

Gynecologic Oncology

journal homepage: www.elsevier.com/locate/ygyno

Exosome transmit the ability of migration and invasion in heterogeneous ovarian cancer cells by regulating autophagy via targeting hsa-miR-328

Hengzi Sun [a,c,1], Xiao Huo [b,c,1], Xiaoning Bi [d], Dongyan Cao [c], Jiaxin Yang [c], Keng Shen [c,*], Peng Peng [c,*]

[a] Department of Obstetrics and Gynecology, Beijing Chao-Yang Hospital, Capital Medical University, Beijing, China
[b] Center of Basic Medical Research, Peking University Third Hospital Institute of Medical Innovation and Research, Beijing, China
[c] Department of Obstetrics and Gynecology, Peking Union Medical College Hospital, Chinese Academy of Medical Sciences and Peking Union Medical College, Beijing, China
[d] Department of Obstetrics and Gynecology, China-Japan Friendship Hospital, Beijing, China

HIGHLIGHTS

- Exosomes from high-migration ovarian cancer cells enhance migration and invasion in low-migration ovarian cancer cells.
- hsa-miR-328-3p targets Raf1, inhibits mTOR, promotes autophagy, and enhances ovarian cancer cell migration and invasion.
- Exosomes carry hsa-miR-328-3p to transmit information between heterogeneous OC cells, regulating autophagy and migration.

ARTICLE INFO

Article history:
Received 18 November 2024
Received in revised form 8 February 2025
Accepted 10 February 2025
Available online xxxx

Keywords:
Ovarian cancer
Exosome
Heterogeneous
Autophagy
Hsa-miR-328

ABSTRACT

Purpose. This study investigates the role of exosomes in ovarian cancer heterogeneity, which contributes to metastasis. By examining the variability of exosomes from different ovarian cancer cells, which aims to elucidate the molecular mechanisms driving this heterogeneity.

Experimental design. Ovarian cancer cell lines were subjected to clonal culture and single-cell sorting. Monoclonal cell lines with different migration and invasion capabilities were identified using Transwell assays. The effect of exosomes on these abilities was assessed through Transwell, scratch tests, and in vivo experiments. High-throughput sequencing was used to compare miRNAs in exosomes with mRNAs in cells. Techniques like electron microscopy, immunofluorescence, adenoviral transduction, western blot, RNA-binding protein immunoprecipitation, and fluorescence in situ hybridization were employed to explore how exosomes affect cell migration and invasion.

Results. Two subpopulations, SK-H/A-H (highly invasive) and SK-L/A-L (less invasive), were isolated. Exosomes from SK-H and A-H cells enhanced the migration and invasion of SK-L and A-L cells. Hsa-miR-328-3p was significantly upregulated in exosomes from SK-H and A-H cells, promoting invasive traits in SK-L and A-L cells, reducing Raf1 and mTOR expression, and increasing ULK1 and LC3B levels to promote autophagy. Overexpression of pri-miR-328-3p in SK-L and A-L cells resulted in similar effects.

Conclusions. Ovarian cancer cells with different invasive capabilities secrete distinct exosomes. Exosomes from highly invasive cells enhance these traits in less aggressive cells via hsa-miR-328-3p, which targets Raf1, disrupts the mTOR pathway, and promotes autophagy. This study highlights exosomes as carriers of hsa-miR-328-3p, mediating intercellular communication and autophagy to influence ovarian cancer cell heterogeneity.

1. Introduction

Ovarian epithelial cancer, the most lethal gynecological malignancy, has a 5-year survival rate of 20–40 % [1]. Key factors influencing treatment efficacy include the extent of surgical resection and chemotherapy response, with metastasis affecting resection completeness. Tumor heterogeneity plays a key role in metastasis. In ovarian cancer, the variability in cell migration and invasion influences patient staging,

* Corresponding authors at: Department of Obstetrics and Gynecology, Peking Union Medical College Hospital, No. 1 ShuaiFuYuan, Dongcheng District, Beijing 100730, China.
E-mail addresses: shenkengpumc@163.com (K. Shen), pengp1999@163.com (P. Peng).
[1] The first two authors contributed equally.

https://doi.org/10.1016/j.ygyno.2025.02.011
0090-8258/

postoperative complications, surgery satisfaction, and the effectiveness of chemotherapy. The role of tumor heterogeneity encompasses both the individual effects of heterogeneous cells and their interactions [2]. However, the mechanisms of interaction between heterogeneous tumor cells are unclear, and no effective therapies target these interactions. Research suggests that metastasis heterogeneity arises from the physical and genetic divergence of distinct tumor populations over time [3]. Cancer may originate from cells with stem cell-like characteristics, with environmental and genetic factors contributing to ovarian cancer stem cell heterogeneity. Research shows that interactions with mesenchymal stem cells can enhance cell adhesion and invasion signaling in cancer cells [4].

Historically, ovarian cancer metastasis was traditionally thought to involve tumor cell detachment and migration through ascitic fluid. However, recent research shows that tumor cells in ascitic fluid are heterogeneous and exposed to a mix of cytokines and exosomes from other tumor cells. These exosomes carry proteins like CD24 and apoptosis-inducing proteins FasL and TRAIL, influencing tumor cells in various ways [5]. Exosomes play a key role in tumor metastasis and are recognized for their potential in disease diagnosis, monitoring, and treatment. They exhibit heterogeneity, with components varying based on their cellular origin, even within exosomes from the same cell line [6]. Our preliminary research has revealed that exosomes secreted by different types of ovarian cancer cell lines contain distinct informational content [7]. Exosomes from ovarian cancer cells with varying migratory and invasive capabilities may reflect the parent cell's traits or contribute to the maintenance of this heterogeneity. Understanding the link between exosomes and ovarian cancer cell invasiveness could improve diagnosis, treatment, and prognosis.

2. Materials and methods

The human epithelial ovarian cancer cell lines SKOV3 and A2780 were obtained from the Institute of Basic Medical Sciences, Chinese Academy of Medical Sciences, and the School of Basic Medicine, Peking Union Medical College. Single-cell subclones were isolated using the limiting dilution method. Cell invasion, migration, and wound-healing assays were conducted to assess the migration and invasion characteristics. Exosomes were isolated from the culture medium using ultracentrifugation. Various techniques, including high-throughput sequencing, Western blot analysis, mouse xenograft experiments, immunohistochemical staining, electron microscopy, immunofluorescence, dual-labeled adenovirus, dual-luciferase reporter assays, miRNA-biotin pull-down, and fluorescence in situ hybridization, were employed to investigate and evaluate the biological mechanisms in ovarian cancer. Primer design and sequence analysis were performed using Primer Premier 6 software. Each experiment was performed in triplicate, and results are expressed as means ± standard deviations (SDs). Statistical significance is denoted in histograms, with * indicating $p < 0.05$, ** indicating $p < 0.01$, and *** indicating $p < 0.001$. A p-value <0.05 was considered statistically significant. Detailed materials and methods are provided in Supplementary Materials S1.

3. Results

3.1. Exosomes secreted by high migratory and invasive ovarian cancer cell lines can enhance the migration and invasion capabilities of low migratory and invasive ovarian cancer cells

In present study, 86 monoclonal cell strains of SKOV3 (SK1-SK86) and 73 of A2780 (A1-A73) were successfully isolated in ovarian cancer cell lines. Following repeated Transwell chamber invasion and migration experiments, SK-8 and SK-9 from SKOV3 strains, and A29 and A32 from A2780 strains were identified as having the most significant differences in invasion and migration capabilities. These were named SK-H (high invasion and migration) and SK-L (low invasion and migration), and A-H (high invasion and migration) and A-L (low invasion and migration) respectively. Experiments were conducted within 50 cell generations to ensure monoclonal cell stability (Supplementary materials S2).

Transmission electron microscopy revealed that the exosomes obtained by ultracentrifugation had a typical lipid bilayer structure, uniformly sized between 30 and 120 nm. Western blot analysis showed positive expression of exosomal markers ALIX, CD63, CD9, and TSG101, and negative expression of GRP94 in all cell strain-derived exosomes. Dynamic observation of ovarian cancer cells engulfing exosomes under confocal microscope showed that all ovarian cancer cell lines were capable of phagocytizing exosomes secreted by ovarian cancer cells, with the intracellular exosomes reaching a dynamic equilibrium after 4 h (Supplementary materials S3).

We evaluated the impact of exosomes from ovarian cancer cell lines SK-L (SK-Lexo), SK-H (SK-Hexo), A-L (A-Lexo), and A-H (A-Hexo) on the migration and invasion of SK-L and A-L cells. Migration and invasion were assessed after treatment with varying concentrations of SK-Lexo and SK-Hexo. Experimental groups included SK-L cells treated with SK-Hexo (50 μg, 100 μg, 200 μg) and A-L cells with A-Hexo (50 μg, 100 μg, 200 μg), while control groups included SK-L and A-L cells treated with their respective exosomes (100 μg, 200 μg). PBS-treated cells served as negative controls. Results showed a dose-dependent increase in migration and invasion with heterologous exosomes. Transwell chamber and Scratch assay experiments confirmed that SK-Hexo and A-Hexo significantly enhanced migration and invasion of SK-L and A-L cells (Fig. 1A, B, Supplementary materials S4 and S5). In animal xenograft models, introduction of high invasion and migration cell strain-derived exosomes resulted in a marked increase in the migration and invasion capabilities of low invasion and migration cell strains (Supplementary materials S6). Moreover, after addition of 200 μg SK-Lexo, there was no significant change in the migration (388.4 ± 65.47 vs. 356.2 ± 77.13, $p > 0.05$) and invasion (123.3 ± 44.74 vs. 108.6 ± 35.05, $p > 0.05$) abilities of SK-H (Supplementary materials S6D).

3.2. High-throughput sequencing analysis revealed that hsa-miR-328-3p may be involved in the transmission process of migratory and invasive heterogeneity in ovarian cancer cells through autophagy

The miRNA sequencing involved experimental groups (SK-Hexo and A-Hexo) and control groups (SK-Lexo and A-Lexo), while mRNA sequencing compared SK-L cells treated with SK-Hexo (SK-L + SK-Hexo) against those treated with SK-Lexo (SK-L + SK-Lexo), and similarly for A-L cells treated with A-Hexo (A-L + A-Hexo) vs. A-Lexo (A-L + A-Lexo).

Our comparative analysis of miRNA expression profiles between SK-Hexo, SK-Lexo, A-Hexo, and A-Lexo unveiled differential expression patterns, identifying 31 and 299 unique miRNAs in the pairwise comparisons (Fig. 1C and Supplementary materials S7). We identified 20 miRNAs consistently differentially expressed between high and low invasive exosomes across both cell lines. Of these, 4 were upregulated and 4 downregulated, suggesting their potential as biomarkers or therapeutic targets for ovarian cancer invasion and migration (Supplementary materials S7).

We identified 3422/3691 mRNAs upregulated and 3532/3843 downregulated across both cell lines after treatment with high-invasive cell-derived exosomes (SK-Hexo, A-Hexo), demonstrating the significant impact of exosomal cargo on gene expression (Fig. 1D, Supplementary materials S8). Integrating data from Miranda and RNAhybrid databases, we identified hsa-miR-328-3p as a shared regulatory miRNA, upregulated in SK-L + SK-Hexo and A-L + A-Hexo conditions. This miRNA targeted 70 downregulated genes in SK-L + SK-Hexo and 63 in A-L + A-Hexo, with 25 common targets (Fig. 1E). Gene Set Enrichment Analysis (GSEA) showed these genes affect PI3K-Akt, mTOR, and p53 pathways, particularly related to autophagy (Fig. 1F, G), with mTOR pathway modulation by key miR-328-3p targets such as RAF1 and ITGB5 (Fig. 1H).

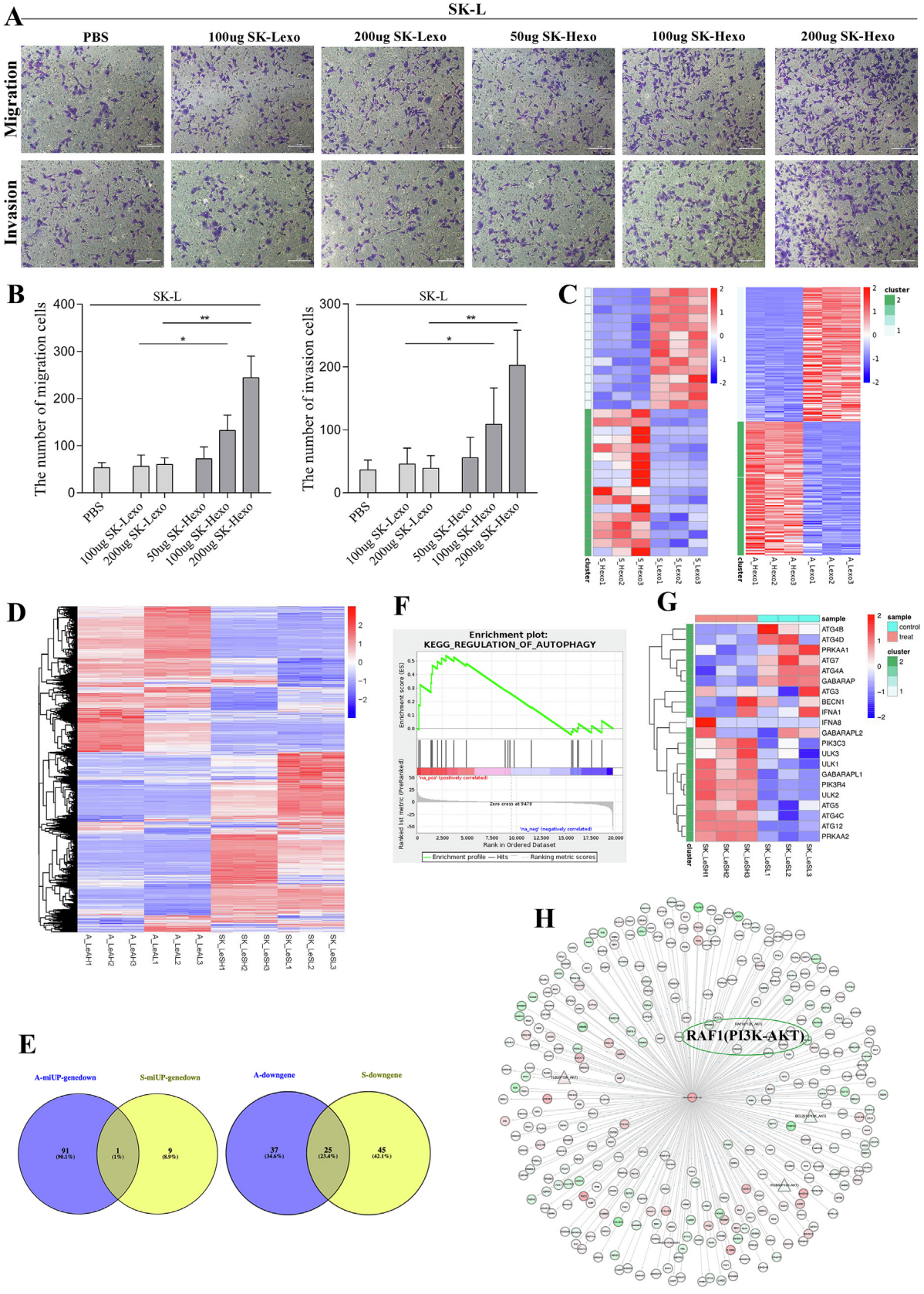

Fig. 1. Effects of exosomes from heterogeneous ovarian cancer cells on the biological behavior of low-invasive ovarian cancer cells, with an exploration of mechanisms. (A, B) Transwell assays assessing the impact of diverse exosomes on ovarian cancer cells. (C) Heatmap showing differentially expressed miRNAs. (D) Overlap of differentially expressed miRNAs affecting gene regulation and targets commonly downregulated by hsa-miR-328-3p. (E) Gene set enrichment analysis (GSEA) of hsa-miR-328-3p target genes. (F) Heatmap of mRNA expression differences between two ovarian cancer cell groups. (G) Gene Ontology (GO) tree of differentially expressed genes. (H) Network diagram of interactions between hsa-miR-328-3p and its target genes. Significance indicated by * ($p < 0.05$) and ** ($p < 0.01$).

3.3. Validation of bioinformatics analysis results through molecular techniques

The SK-H, SK-L, A-H, and A-L cells, along with their secreted exosomes SK-Hexo, SK-Lexo, A-Hexo, and A-Lexo, were systematically collected. Subsequently, the expression of hsa-miR-328-3p was examined using qRT-PCR. The results revealed a significant upregulation of hsa-miR-328-3p expression in SK-H, A-H, SK-Hexo, A-Hexo, SK-L + SK-Hexo and A-L + A-Hexo (Fig. 2A). The western blot demonstrated a notable decrease in Raf1 and mTOR expression in SK-L post-SK-Hexo treatment, accompanied by an increase in ULK1 and LC3B II expression (Fig. 2B).

4. The overexpression of hsa-miR-328-3p demonstrates an augmentation in the migratory and invasive capabilities of SK-L cells

4.1. Verification of overexpression/inhibition of hsa-miR-328-3p by qRT-PCR

To substantiate the functional implications of hsa-miR-328-3p, miRNA mimics were transfected into SK-L and A-L cell lines to induce overexpression of hsa-miR-328-3p. The efficacy of transfection and subsequent overexpression was assessed using qRT-PCR. The results indicated a significant upregulation of hsa-miR-328-3p expression post-transfection, with an approximate eight-fold increase in the SK-L cell line and a five-fold increase in the A-L cell line (Fig. 2C). After transfection with miR-328-3p inhibitor, the expression of hsa-miR-328-3p was significantly decreased in SK-H and SK-L + SK-Hexo cells (Supplementary materials S6D).

4.2. Transwell and Wound healing assays

Upon overexpression of hsa-miR-328-3p, both SK-L and A-L cell lines demonstrated a significant enhancement in their migratory and invasive capabilities. The data indicate that the number of cells migrating to the lower chamber increased substantially in both cell lines upon transfection with miR-328-3p mimics compared to control mimics. Specifically, the migration numbers were as follows: SK-L + control mimics at 75.8 ± 25.33, SK-L + miR-328-3p mimics at 373.4 ± 75.35, A-L + control mimics at 35.4 ± 16.32, and A-L + miR-328-3p mimics at 223.5 ± 63.44. Similarly, the invasion assays revealed a marked increase in the number of cells invading through the matrix to the lower chamber (Fig. 2D). The wound healing assay demonstrate a significant increase in migration width 24 h post-scratch in both cell lines transfected with miR-328-3p mimics compared to those transfected with control mimics ($p < 0.01$) (Fig. 2E). The Transwell assays also showed the numbers of migrated and invaded cells in the SK-L + SK-Hexo groups have re-decreased after inhibition of hsa-miR-328-3p (145.3 ± 42.54 vs. 56.2 ± 15.69, $p < 0.01$; 103.3 ± 44.74 vs. 36.58 ± 12.77, $p < 0.01$) (Supplementary S6E). The Transwell migration and invasion assays showed the numbers of migrated and invaded cells in the SK-H groups have decreased after inhibited the expression of hsa-miR-328-3p (315.0 ± 31.22 vs. 151.2 ± 56.75, $p < 0.01$; 115.0 ± 21.22 vs. 46.58 ± 22.77, $p < 0.01$) (Supplementary materials S6D).

5. hsa-miR-328-3p enhances the metastatic and invasive capabilities of ovarian cancer cells through the regulation of autophagy

5.1. Verification of target gene expression by western blot analysis

In present study, after transfecting with miR-328-3p mimics, the expression of target genes and related pathway genes was assessed in SK-H, SK-L, SK-L + miR-328-3p mimics, and SK-L + control mimics. Results showed a significant decrease in RAF1 and mTOR expression following miR-328-3p mimic transfection. Conversely, ULK1 and the autophagy protein LC3B were significantly upregulated, while ATG5 expression increased and the autophagy substrate protein p62 decreased (Fig. 2B). The Western blot results demonstrated a notable upregulation in the expression levels of RAF1 and mTOR following transfection with the hsa-miR-328-3p inhibitor in highly invasive cells (SK-H). Conversely, a marked upregulation in the expression of ULK1 and the autophagy core protein LC3B was observed. Additionally, the levels of autophagy-related proteins ATG5 and ATG7 were elevated, while the expression of the autophagy substrate protein p62 was notably decreased (Supplementary materials S6F).

5.2. Observation of autophagosomes by electron microscopy after transfection with miR-328-3p

Following the transfection with miR-328-3p, an increase in the expression of the autophagy core protein LC3B was observed, suggesting enhanced autophagic activity. Consequently, electron microscopy was employed to examine the cells post-transfection, revealing a notable increase in the number of autophagosomes within the cells (Fig. 3A).

5.3. Verification of autophagy expression by immunofluorescence after transfection with miR-328-3p

The enhancement of autophagy following the transfection with miR-328-3p mimics was further validated using immunofluorescence. The assay revealed a significant increase in the expression of the autophagy core protein LC3B, which exhibited a clustered distribution pattern within the cells. This pattern indicates an intensification of autophagic processes (Fig. 3B).

5.4. Assessment of autophagy expression using LC3B-GFP/lysosome-mCherry dual-label adenovirus after transfection with miR-328-3p

To further investigate the impact of miR-328-3p on autophagy, a dual-label adenovirus expressing LC3B-GFP and lysosome-mCherry was employed to monitor autophagic activity in cells transfected with miR-328-3p mimics. This advanced technique allows for the simultaneous visualization of autophagosomes (marked by LC3B-GFP) and lysosomes (marked by lysosome-mCherry), facilitating the observation of autophagy in real-time. The findings revealed an increase in the co-localization of autophagosomes with lysosomes, indicative of enhanced autophagic flux. This increase suggests that the transfection with miR-328-3p mimics not only augments the formation of autophagosomes but also promotes their fusion with lysosomes, thereby enhancing the autophagic degradation process (Fig. 3C).

5.5. Assessing cell migration and invasion following overexpression of hsa-miR-328-3p and silencing of LC3B

To investigate the impact of LC3B silencing on cell migration and invasion after overexpressing hsa-miR-328-3p, SK-L and A-L cells were transfected with siLC3B, and successful silencing was confirmed by Western blot, showing a significant reduction in LC3B protein levels (Fig. 3D). Overexpression of hsa-miR-328-3p in SK-L cells significantly altered migration and invasion. Quantification of cell migration to the lower chamber showed that SK-L cells with miR-328-3p mimics in wild-type conditions migrated 388.4 ± 65.47 cells. Migration slightly decreased with non-targeting control siRNA (siNC) to 356.2 ± 77.13 cells and dropped to 151.2 ± 56.75 cells with LC3B silencing. Control mimics showed significantly lower migration rates (68.6 ± 31.22 for WT, 79.4 ± 38.16 for siNC, 74.7 ± 24.36 for siLC3B), with invasion assays confirming these results (Fig. 3E).

5.6. Fluorescent in situ hybridization (FISH) analysis in high-grade serous ovarian cancer tumor tissues

This study included 10 patients with Stage IIIC high-grade serous ovarian cancer treated at Peking Union Medical College Hospital

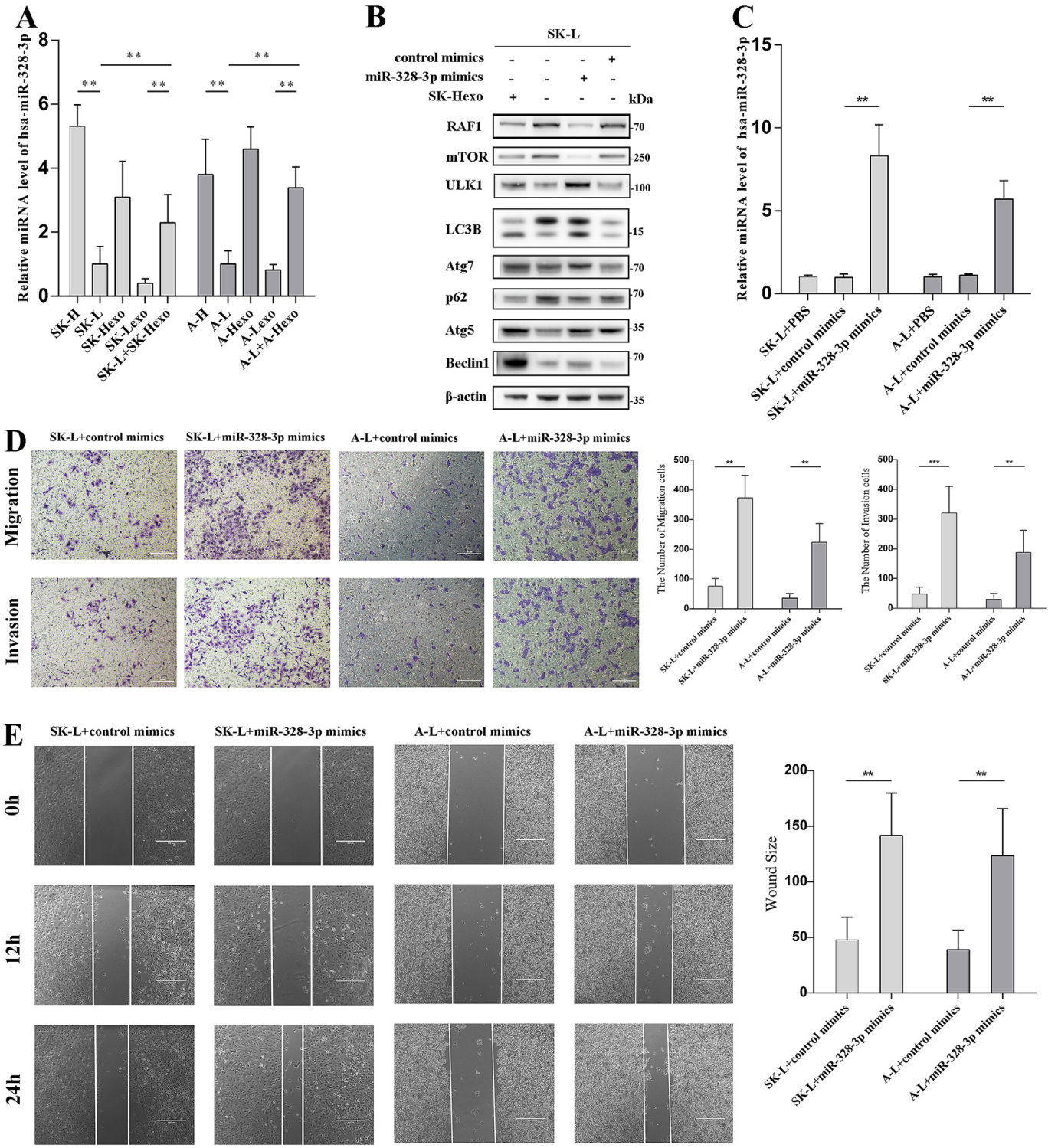

Fig. 2. Validation of bioinformatics predictions. (A) qRT-PCR validation of differentially expressed miRNAs. (B) Western blot analysis confirms differential mRNA expression. (C) qRT-PCR verification of hsa-miR-328-3p overexpression. (D, E) Transwell and wound healing assays assessing the impact of hsa-miR-328-3p on cellular behavior. Significance levels are denoted as ** ($p < 0.01$).

between December 2017 and December 2018. Tumor tissue blocks from primary and peritoneal metastatic sites were paired for fluorescent in situ hybridization (FISH) analysis of hsa-miR-328-3p and LC3B. The results showed that in 4 out of 10 cases, hsa-miR-328-3p and LC3B expression levels were significantly higher in metastatic tissue compared to primary lesions (Fig. 3F).

5.7. Evaluation of hsa-miR-328-3p's impact on the migration and invasion capabilities of ovarian cancer cells in a xenograft model

Experimental groups using SK-L/miR-328-3p-luc and A-L/miR-328-3p-luc cell lines were compared to control groups with SK-L/miRcontrol-luc and A-L/miRcontrol-luc cells. These cells were

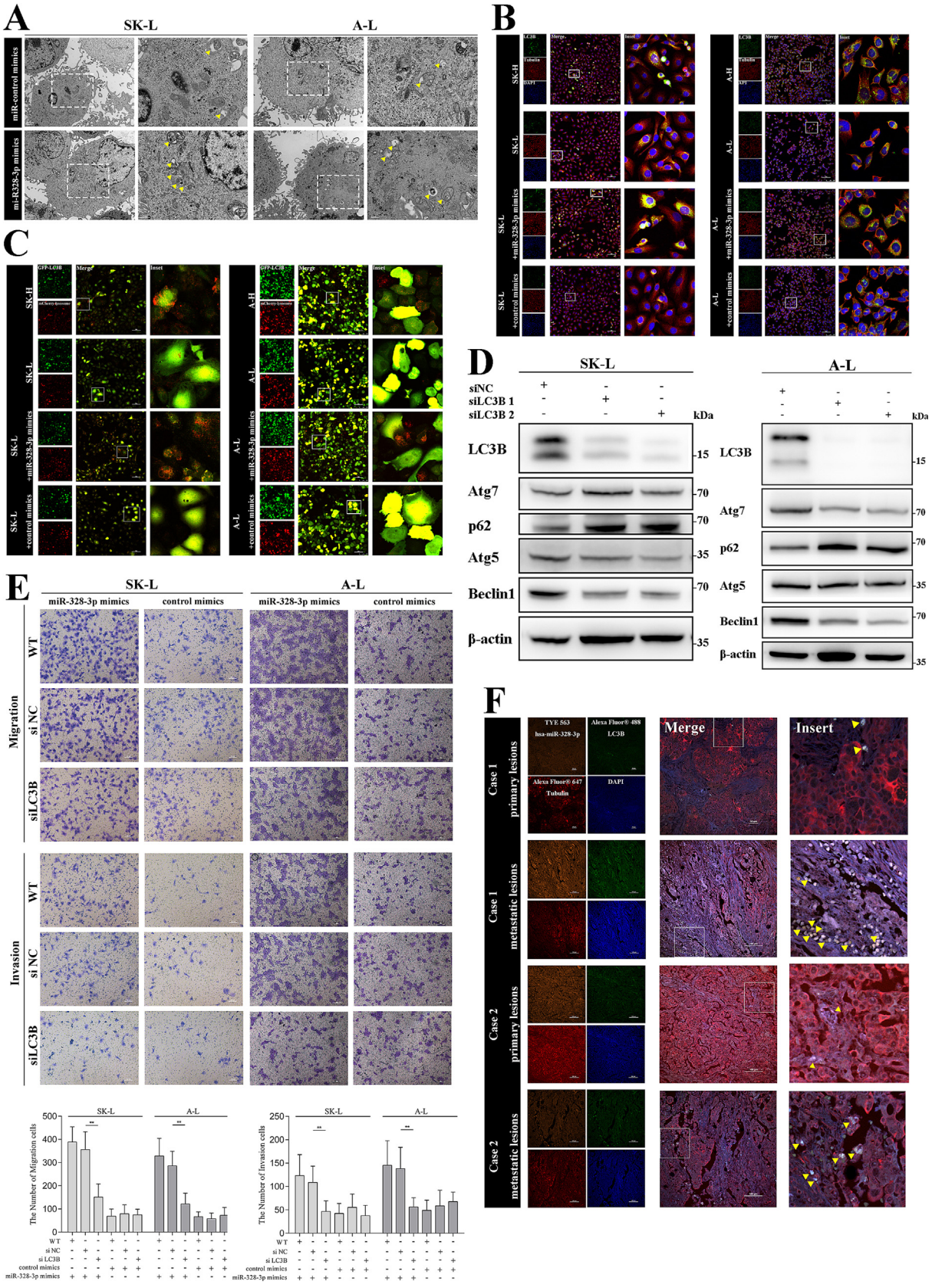

Fig. 3. Enhancement of metastatic and invasive capabilities in ovarian cancer cells by hsa-miR-328-3p via autophagy regulation. (A) Electron microscopy images of autophagosomes. (B) Immunofluorescence analysis for autophagy markers. (C) Measurement of autophagy levels using a dual-labeled adenovirus. (D) Western blot analysis confirming expression of target genes. (E) Transwell assays to evaluate cell migration and invasion. (F) Fluorescence in situ hybridization (FISH) to assess autophagy marker expression. Significance indicated by ** ($p < 0.01$).

implanted into the peritoneal cavities of nude mice ($N = 6$/group) and cultivated for 40 days. In vivo imaging showed a significant increase in tumor metastasis in the experimental groups, with metastatic counts of 5.2 ± 1.6 and 4.8 ± 2.0 for SK-L/miR-328-3p-luc and A-L/miR-328-3p-luc, respectively, compared to 1.4 ± 0.7 and 1.6 ± 0.4 in the controls ($p < 0.05$) (Fig. 4A, B). H&E staining and immunohistochemistry confirmed the enhanced migration and invasion abilities of the miR-328-3p-overexpressing cells (Fig. 4C, D).

6. Exploring the mechanism of action of hsa-miR-328-3p

6.1. Dual-luciferase reporter assay validation

TargetScan was used to predict the binding position and complementary sequences of hsa-miR-328-3p in the 3'-UTR of RAF1. The dual-luciferase reporter assay was employed to validate the post-transfection effects of hsa-miR-328-3p on cellular luciferase expression.

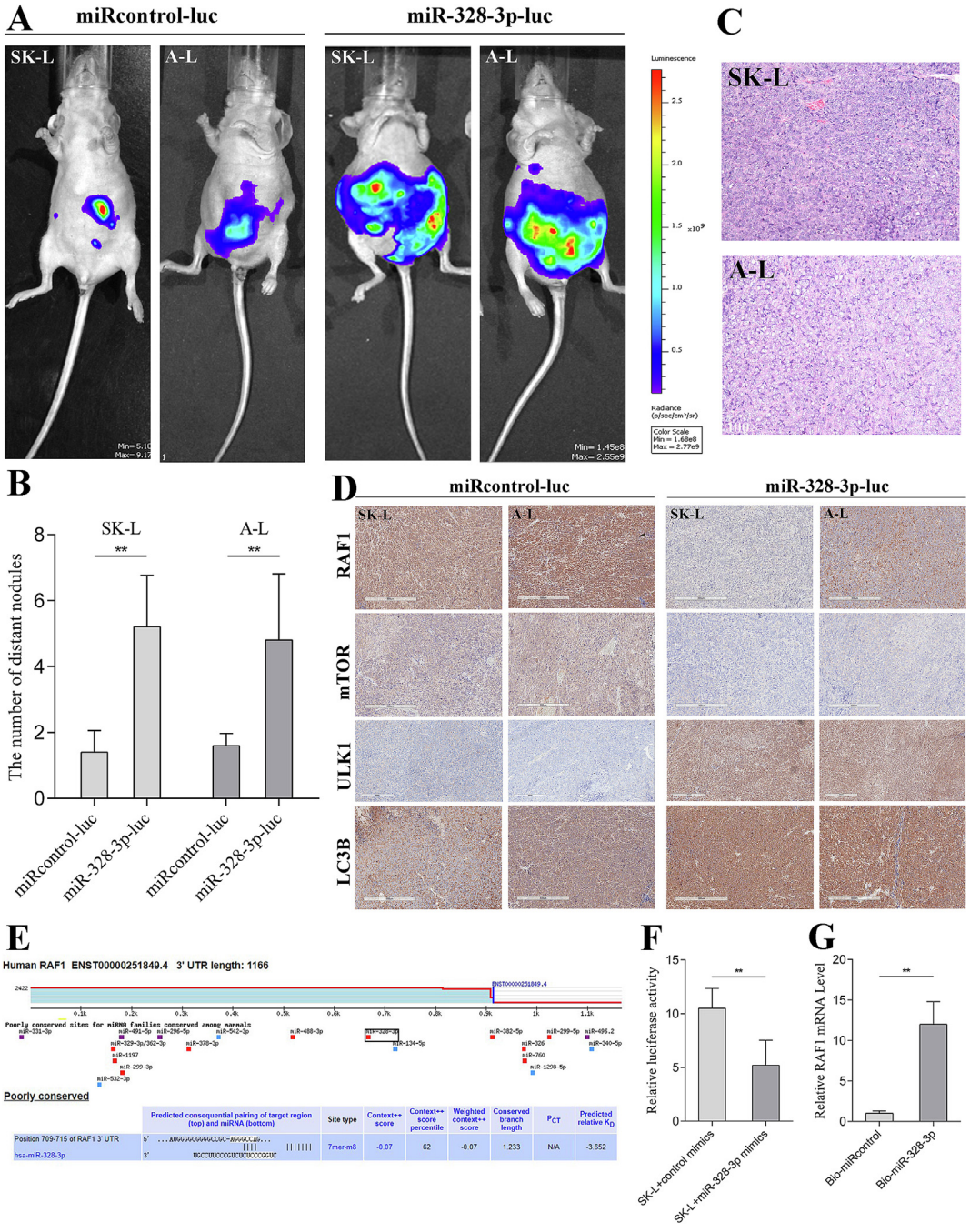

Fig. 4. Functional analysis and mechanistic insights into hsa-miR-328-3p action. (A, B) Evaluation of hsa-miR-328-3p in a xenograft model. (C) Hematoxylin and eosin (H&E) staining (100×). (D) Immunohistochemical validation of hsa-miR-328-3p-regulated target and pathway genes. (E) Identification of hsa-miR-328-3p binding sites and complementary sequences in RAF1 3'-UTR as predicted by TargetScan. (F) Luciferase reporter assays of RAF1 3'-UTR with miR-328-3p mimics or control in SK-L cells; luciferase activity measured after 48 h. (G) Measurement of RAF1 levels recruited by Bio-miR-328-3p or control probes via miRNA pull-down assay. Significance indicated by ** ($p < 0.01$).

Following the transfection with hsa-miR-328-3p, a significant reduction in luciferase expression was observed, confirming the ability of hsa-miR-328-3p to bind to the promoter region of RAF1 and consequently regulate its expression (Fig. 4E, F).

6.2. Verification of the interaction between hsa-miR-328-3p and RAF1 mRNA through pull-down assay

The specific binding between hsa-miR-328-3p and RAF1 mRNA was validated utilizing a pull-down assay technique. Biotin-labeled hsa-miR-328-3p (Bio-miR-328-3p) was transfected into cells, enabling the isolation of mRNA that binds specifically to the b Bio-miR-328-3p. The binding products were then examined using quantitative reverse transcription PCR (qRT-PCR). Compared to the control group, a significant increase in RAF1 expression was observed in the products bound to Bio-miR-328-3p, confirming the direct interaction between hsa-miR-328-3p and RAF1 mRNA (Fig. 4G).

7. Validation of exosomes as miRNA carriers for intercellular communication

7.1. Construction of luciferase-tagged pri-miR-328-3p and transfection into stable cell lines labeled with YFP-tagged CD63

Lentiviral vectors were used to engineer low metastatic ovarian cancer cell lines (SK-L and A-L) to co-express pri-miR-328-3p-luciferase and CD63-YFP. Stable cell lines were established after puromycin selection. The experimental groups were SK-L/pri-miR-328-3p-luc-CD63-YFP and A-L/pri-miR-328-3p-luc-CD63-YFP, while the controls included SK-L/pri-miRcontrol-luc-CD63-YFP, SK-L/pri-miR-328-3p-luc-control-YFP, A-L/pri-miRcontrol-luc-CD63-YFP, and A-L/pri-miR-328-3p-luciferase-control-YFP. qRT-PCR analysis showed a significant increase in both pri-miR-328 and its mature form in the experimental groups ($p < 0.01$), confirming successful transfection (Fig. 5A).

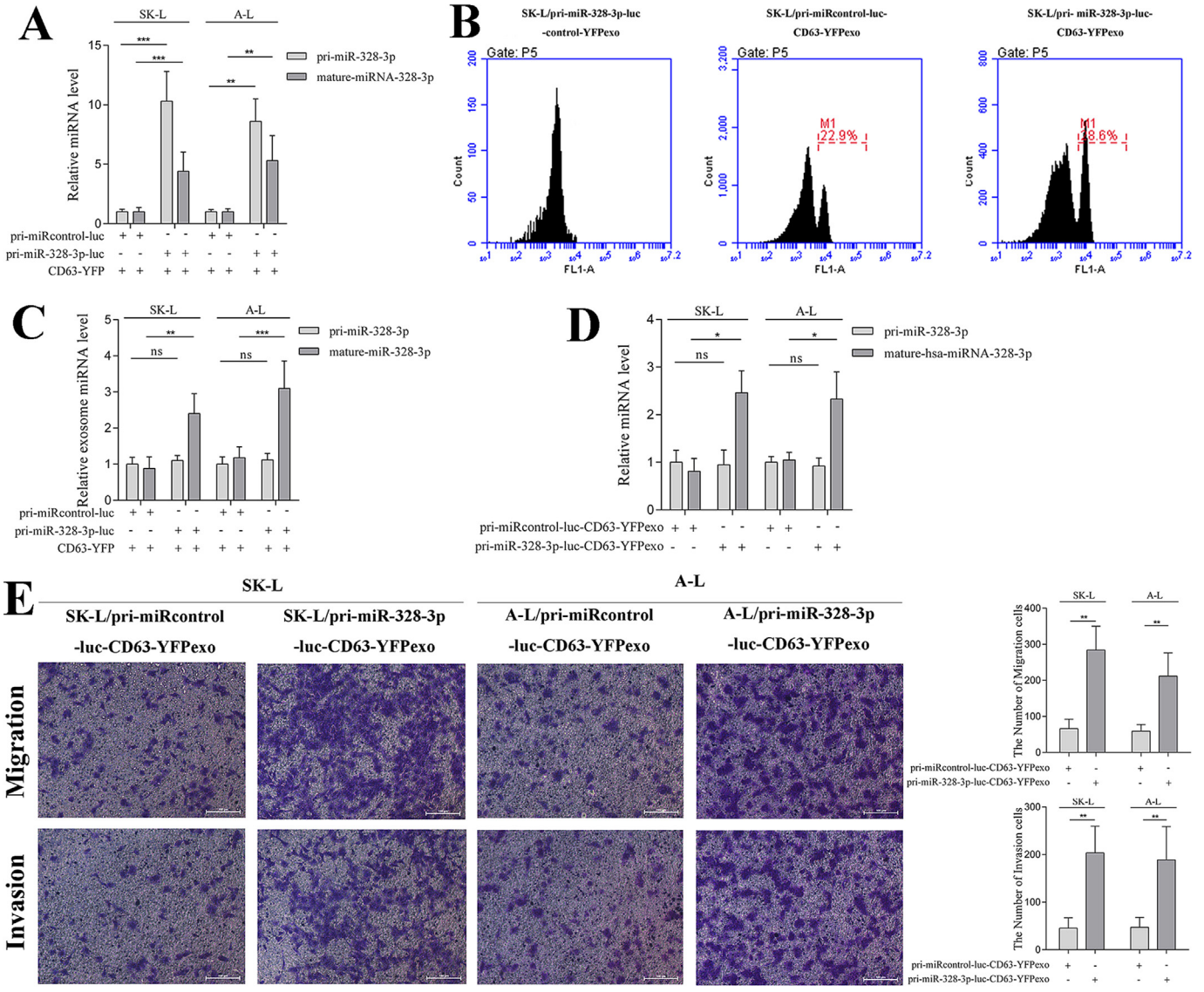

Fig. 5. Validation of exosomes as miRNA carriers in intercellular communication. (A) Quantification of transfection efficiency and expression levels of pri-miR-328 and its mature form in YFP-tagged CD63-positive cells via qRT-PCR. (B) Flow cytometry analysis of exosomes secreted by cells transfected with CD63-YFP. (C) qRT-PCR analysis of miRNA expression in CD63-YFP positive exosomes sorted by flow cytometry. (D) qRT-PCR detection of pri-miR-328-3p and its mature form in cells after co-cultivation with sorted exosomes. (E) Transwell assays to assess cell migration and invasion following co-cultivation with sorted exosomes. Significance levels are denoted as ns ($p > 0.05$), * ($p < 0.05$), ** ($p < 0.01$) and *** ($p < 0.001$).

7.2. Expression of primary miRNA and its mature form in exosomes from various cell groups was assessed using flow cytometry sorting and qRT-PCR

Flow cytometry analysis of exosomes from cells transfected with CD63-YFP identified two distinct populations, with exosomes containing YFP making up about 30 % of the total (Fig. 5B). After sorting these exosomes, sterile filtration was used for purification. qRT-PCR analysis of the sorted exosomes showed that pri-miR-328-3p expression did not significantly differ between exosomes from SK-L/pri-miR-328-3p-luc-CD63-YFP and A-L/pri-miR-328-3p-luc-CD63-YFP cell lines and control groups. However, the mature form of hsa-miR-328-3p was significantly increased ($p < 0.01$, $p < 0.001$, Fig. 5C).

7.3. After administering sorted exosomes to cells, the expression of primary and mature miRNA and their biological functions were assessed

qRT-PCR analysis of pri-miR-328-3p and its mature form in cells co-cultivated with exosomes for 48 h showed no significant difference in pri-miR-328-3p expression between experimental and control groups. However, mature hsa-miR-328-3p expression was significantly increased ($p < 0.05$, Fig. 5D). Transwell assays revealed enhanced migration and invasion in SK-L and A-L cells after exosome treatment. SK-L cells treated with SK-L/pri-miR-328-3p-luc-CD63-YFP exosomes showed significantly higher migration (284.3 ± 65.90) compared to control (66.3 ± 25.88), and similar results were observed in A-L cells (211.7 ± 64.34 vs. 59.1 ± 18.29) ($p < 0.01$, Fig. 5E). These findings were confirmed in xenograft models, where control groups showed fewer tumor metastases ($p < 0.05$, Supplementary materials S9A—D). Exosomes from low-invasive cells overexpressing pri-miR-328-3p enhanced their migratory and invasive abilities.

7.4. Evaluation of target gene expression by western blot analysis

Following a 48-h treatment with exosomes, western blot analysis was conducted to evaluate the expression of key genes within specific pathways in cells treated with SK-L + SK-L/pri-miRcontrol-luc-CD63-YFP exosomes, SK-L + SK-L/pri-miR-328-3p-luc-CD63-YFP exosomes, A-L + A-L/pri-miRcontrol-luc-CD63-YFP exosomes, and A-L + A-L/pri-miR-328-3p-luc-CD63-YFP exosomes. The results demonstrated a significant reduction in the expression of RAF1 and mTOR in cells treated with SK-L + SK-L/pri-miR-328-3p-luc-CD63-YFP exosomes and A-L + A-L/pri-miR-328-3p-luc-CD63-YFP exosomes, compared to controls. Furthermore, there was a notable increase in the expression of ULK1 and the autophagy core protein LC3B, as well as the autophagy-related protein ATG5. The expression of the autophagy substrate protein p62 was observed to decrease (Supplementary materials S9E).

7.5. Validation of the impact of exosomes on cellular autophagy

Cellular immunofluorescence analysis showed that treatment with exosomes from the experimental groups SK-L + SK-L/pri-miR-328-3p-luc-CD63-YFPexo and A-L + A-L/pri-miR-328-3p-luc-CD63-YFPexo led to a significant increase in LC3B expression, with a clustered distribution, indicating enhanced cellular autophagy. This effect intensified with higher exosome concentrations (Supplementary S9F). Dual-label adenovirus expressing LC3B-GFP and lysosome-mCherry revealed increased autophagic lysosomes in the experimental groups, further suggesting enhanced autophagic activity (Supplementary S9G).

8. Discussion

Over the past three decades, despite advances in therapeutic strategies and technology, the mortality rate of ovarian cancer has only marginally decreased. This is primarily due to the fact that nearly 60 % of cases are diagnosed at an advanced stage due to the absence of overt symptoms and effective screening strategies [8]. The standard treatment for advanced ovarian cancer includes cytoreductive surgery followed by chemotherapy, but most patients relapse within two to three years due to metastasis and chemoresistance, losing the chance for further treatment. Tumor heterogeneity plays a key role in metastasis, recurrence, and therapy resistance. As tumors progress, genetic mutations lead to their evolution from monoclonal to polyclonal states, with significant differences among tumor cell subpopulations in morphology, protein expression, and genetic traits. Cells with advantageous mutations gain enhanced metastatic potential, often becoming the source of recurrence [9–13]. To minimize the impact of genetic background differences on research outcomes, this study selected the SKOV3 cell line derived from the ascites of ovarian cancer patients and the A2780 cell line from primary tumor sites. We successfully isolated and established two pairs of cell subclones with differing migratory and invasive capabilities, providing a robust model for studying intratumoral heterogeneity in ovarian cancer due to their identical genetic backgrounds.

Recent advancements have emphasized the role of exosomes in mediating cellular functions through miRNA delivery. In biological systems, miRNA genes are transcribed into primary miRNAs (pri-miRNAs), processed by the Drosha complex into precursor miRNAs (pre-miRNAs), and transported to the cytoplasm by exportin-5. Pre-miRNAs are then further processed by the Dicer complex into mature miRNAs. These mature miRNAs are sorted into exosomes via four mechanisms: (1) the nSMase2-dependent pathway, (2) a pathway dependent on miRNA motifs and ubiquitinated hnRNPs, (3) a 3' miRNA sequence-dependent pathway, and (4) the miRISC-related pathway, where components like AGO2 proteins help target miRNAs to exosome biogenesis sites, facilitating their sorting into exosomes [14]. Due to their transportability, miRNAs in exosomes have gained significant attention. Circulating vesicles are considered the third mode of intercellular communication, alongside cell-to-cell contact and soluble molecule signaling [15].

Tumor-secreted miRNAs, including those in exosomes, play a crucial role in metastasis. For instance, exosomes from metastatic breast cancer cells carry miR-10b, increasing invasiveness in non-malignant breast epithelial cells, and miR-105, which disrupts the vascular barrier by targeting ZO-1 mRNA in endothelial cells. In prostate cancer, exosomal miR-21-5p, miR-100-5p, and miR-139-5p promote metastasis by enhancing MMP expression in fibroblasts. In ovarian cancer, exosomal miR-141-3p and miR-205 facilitate metastasis and proliferation [16–21]. Our study found miR-328-3p in exosomes from highly invasive ovarian cancer cells significantly enhances migration and invasion in less invasive cells. MiR-328 influences processes like migration, invasion, and proliferation, activating pathways such as Wnt, PI3K/AKT, and MAPK, and promoting EMT [22]. Previous studies have demonstrated elevated levels of miR-328 in ovarian cancer, correlating with a poorer prognosis [23]. However, the specific mechanisms by which miR-328 operates in ovarian cancer remain to be fully elucidated. Autophagy is a conserved catabolic process that targets cellular contents for lysosomal degradation and is significantly linked to tumor metastasis. Increased punctate staining of the autophagy core protein LC3B correlates with lymph node metastasis and poorer survival in human breast cancer. In metastatic melanoma, LC3B staining is notably higher than in primary tumor samples. Similarly, in hepatocellular carcinoma, LC3B expression is higher in metastatic sites compared to primary lesions, with early metastases showing even greater expression. In glioblastoma, high autophagy gene expression leads to increased migration and invasiveness. Autophagy affects cellular migration by regulating RhoA and its downstream signals and plays a direct role in focal adhesion dynamics. Sharifi et al. found that inhibiting autophagy reduced tumor cell migration and invasion in metastatic cancer cell lines, suppressing metastasis in an in-situ mouse model through LC3B's interaction with the focal adhesion protein Paxillin. Additionally, inhibiting HSP90s can promote tumor cell invasion by reducing AMPK and ULK1

activity while increasing FAK expression. Autophagy-generated cytokines like IL-6, MMP2, and WNT-5 A are also crucial for tumor cell invasion [24–30]. Furthermore, autophagy-generated cytokines such as interleukin-6 (IL-6), MMP2, and WNT-5 A, as specific factors, are also essential for tumor cell invasion [31].

miR-20a and miR-106b regulate autophagy by inhibiting ULK1 expression in myocytes. miR-338-5p silences the PI3K complex subunit PIK3C3 (Vps34), inhibiting autophagy and promoting colorectal cancer cell migration. miR-30a, miR-376b, and miR-216a target Beclin-1, reducing autophagic activity. miR-17 and miR-375 target ATG7, increasing cancer cell sensitivity to chemotherapy and decreasing hepatocellular carcinoma cell survival under hypoxia. miR-181a, miR-374a, and miR-30a inhibit autophagy by targeting ATG5. Raf1 promotes Rheb expression, activating mTOR and suppressing autophagy. Several miRNAs, including miR-21 and miR-216b, regulate Ras expression, playing roles in tumor suppression [32–39].

Advancements in biomedical technologies have enhanced nanoscale drug delivery systems for cancer treatment, but issues like poor targeting and rapid degradation limit their effectiveness, especially for gene therapies. Exosomes offer advantages as targeted carriers: minimal immune response, good blood stability, efficient cargo delivery, inherent targeting, and the ability to exploit the EPR effect for tumor penetration. Exosome engineering is key for clinical applications, as they can carry various therapeutics, including chemotherapeutics and nucleic acids [40]. This study found that miR-328-3p, delivered via exosomes, targets Raf1, inhibiting mTOR activation, enhancing autophagy, and promoting cell migration and invasion, offering insights into ovarian cancer biology and new therapeutic approaches (Fig. 6).

9. Conclusion

Ovarian cancer cells exhibiting heterogeneous migration and invasion characteristics secrete exosomes that are also heterogeneous in nature. Notably, exosomes from highly migratory and invasive ovarian cancer cells can enhance the migration and invasion capabilities of cells with lower migratory and invasive properties. The present study reveals that exosomes can carry hsa-miR-328-3p, facilitating intercellular communication among heterogeneous ovarian cancer cells. These exosomes target Raf1, inhibit the mTOR pathway, and promote cellular autophagy, thereby augmenting the migration and invasion capabilities of ovarian cancer cells. Understanding this mechanism could provide new directions for the treatment of ovarian cancer.

Supplementary data to this article can be found online at https://doi.org/10.1016/j.ygyno.2025.02.011.

Funding

This study was funded by the Beijing Science and Technology Plan Project [D151100001915004 (Shen Keng)], National Natural Science Foundation of China (81402140) and CAMS Innovation Fund for Medical Sciences (CIFMS) [CAMS-2017-I2M-1-002 (Shen Keng)].

CRediT authorship contribution statement

Hengzi Sun: Writing – original draft, Formal analysis, Conceptualization. **Xiao Huo:** Formal analysis, Conceptualization. **Xiaoning Bi:** Data curation. **Dongyan Cao:** Data curation. **Jiaxin Yang:** Formal analysis,

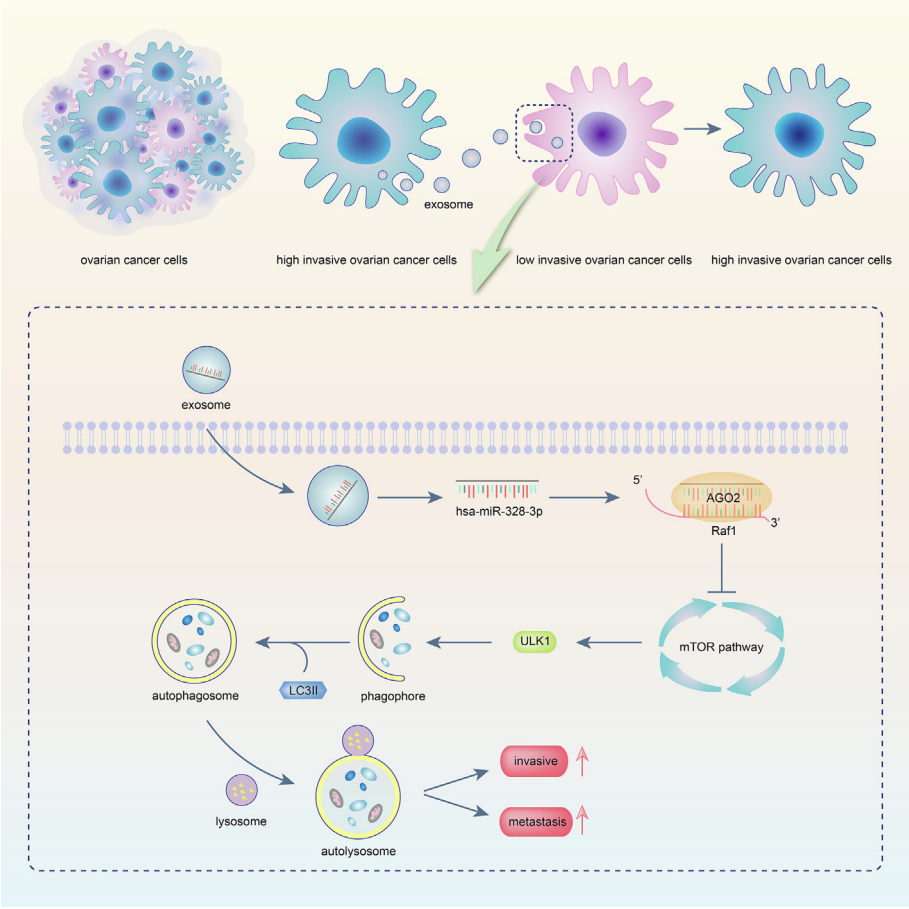

Fig. 6. Schematic diagram of the biological role of the *exo*-miR-328-3p in heterogeneous ovarian cancer.

Data curation. **Keng Shen:** Funding acquisition, Formal analysis, Data curation. **Peng Peng:** Methodology, Data curation, Conceptualization.

Declaration of competing interest

The authors declare that they have no conflicts of interest related to this work.

Acknowledgments

Ethical approval: All procedures in studies involving animals were performed in accordance with the ethical standards of the institutional and national research committee and 3Rs. (Name and affiliation of the approving ethics committee: Institutional Ethics Committee of Peking Union Medical College Hospital, CAMS Chinese Academy of Medical Sciences; No. S-0081 2014). All procedures in studies involving human participants were performed in accordance with the ethical standards of the institutional and national research committee and with the 1964 Helsinki Declaration and its later amendments. (Name and affiliation of the approving ethics committee: Institutional Ethics Committee of Peking Union Medical College Hospital, CAMS Chinese Academy of Medical Sciences; No. S-341 2019). Written informed consent was obtained from all participants included in the study.

References

[1] L.A. Torre, B. Trabert, C.E. DeSantis, K.D. Miller, G. Samimi, C.D. Runowicz, et al., Ovarian cancer statistics, 2018, CA Cancer J. Clin. 68 (4) (2018) 284–296.
[2] L. Nelson, A. Tighe, A. Golder, S. Littler, B. Bakker, D. Moralli, et al., A living biobank of ovarian cancer ex vivo models reveals profound mitotic heterogeneity, Nat. Commun. 11 (2020) 822.
[3] S. Gerstberger, Q. Jiang, K. Ganesh, Metastasis, Cell 186 (2023) 1564–1579.
[4] R. Lis, C. Touboul, N.M. Halabi, A.S. Madduri, D. Querleu, J. Mezey, et al., Mesenchymal cell interaction with ovarian cancer cells induces a background dependent prometastatic transcriptomic profile, J. Transl. Med. 12 (2014) 59.
[5] L. Guo, N. Guo, Exosomes: potent regulators of tumor malignancy and potential biotools in clinical application, Crit. Rev. Oncol. Hematol. 95 (2015) 346–358.
[6] X. Zou, Q. Lei, X. Luo, J. Yin, S. Chen, C. Hao, et al., Advances in biological functions and applications of apoptotic vesicles, Cell Commun. Signal. 21 (2023) 260.
[7] W. Zhang, J. Yang, D. Cao, Y. You, K. Shen, P. Peng, Regulation of exosomes released from normal ovarian epithelial cells and ovarian cancer cells, Tumour Biol. 10 (2016) 0(0).
[8] R.L. Siegel, K.D. Miller, A. Jemal, Cancer statistics, 2018, CA Cancer J. Clin. 68 (2018) 7–30.
[9] P. Dinh, P. Harnett, M.J. Piccart-Gebhart, A. Awada, New therapies for ovarian cancer: cytotoxics and molecularly targeted agents, Crit. Rev. Oncol. Hematol. 67 (2008) 103–112.
[10] M. Gerlinger, A.J. Rowan, S. Horswell, J. Larkin, D. Endesfelder, E. Gronroos, et al., Intratumor heterogeneity and branched evolution revealed by multiregion sequencing, N. Engl. J. Med. 366 (2012) 883–892.
[11] P.C. Nowell, The clonal evolution of tumor cell populations, Science 194 (1976) 23–28.
[12] R. Durrett, J. Foo, K. Leder, J. Mayberry, F. Michor, Intratumor heterogeneity in evolutionary models of tumor progression, Genetics 188 (2011) 461–477.
[13] T. Tanaka, Y. Kuramitsu, M. Fujimoto, S. Naito, M. Oka, K. Nakamura, Downregulation of two isoforms of ubiquitin carboxyl-terminal hydrolase isozyme L1 correlates with high metastatic potentials of human SN12C renal cell carcinoma cell clones, Electrophoresis 29 (2008) 2651–2659.
[14] J. Zhang, S. Li, L. Li, M. Li, C. Guo, J. Yao, et al., Exosome and exosomal microRNA: trafficking, sorting, and function, Genomics Proteomics Bioinforma. 13 (2015) 17–24.
[15] T. Kuroiwa, E.G. Lee, C.L. Danning, G.G. Illei, I.B. McInnes, D.T. Boumpas, CD40 ligand-activated human monocytes amplify glomerular inflammatory responses through soluble and cell-to-cell contact-dependent mechanisims, J. Immunol. 163 (1999) 2168–2175.
[16] R. Singh, R. Pochampally, K. Watabe, Z. Lu, Y.-Y. Mo, Exosome-mediated transfer of miR-10b promotes cell invasion in breast cancer, Mol. Cancer 13 (2014) 256.
[17] W. Zhou, M.Y. Fong, Y. Min, G. Somlo, L. Liu, M.R. Palomares, et al., Cancer-secreted miR-105 destroys vascular endothelial barriers to promote metastasis, Cancer Cell 25 (2014) 501–515.
[18] J. Lan, L. Sun, F. Xu, L. Liu, F. Hu, D. Song, et al., M2 macrophage-derived exosomes promote cell migration and invasion in colon cancer, Cancer Res. 79 (2019) 146–158.
[19] J. Ding, Z. Xu, Y. Zhang, C. Tan, W. Hu, M. Wang, et al., Exosome-mediated miR-222 transferring: an insight into NF-κB-mediated breast cancer metastasis, Exp. Cell Res. 369 (2018) 129–138.
[20] S. Masoumi-Dehghi, S. Babashah, microRNA-141-3p-containing small extracellular vesicles derived from epithelial ovarian cancer cells promote endothelial cell angiogenesis through activating the JAK/STAT3 and NF-kappaB signaling pathways, J. Cell Commun. Signal. 14 (2) (2020) 233–244.
[21] L. He, W. Zhu, Q. Chen, Y. Yuan, Y. Wang, J. Wang, et al., Ovarian cancer cell-secreted exosomal miR-205 promotes metastasis by inducing angiogenesis, Theranostics 9 (2019) 8206–8220.
[22] Z. Wang, W. Xie, H. Guan, The diagnostic, prognostic role and molecular mechanism of miR-328 in human cancer, Biomed. Pharmacother. 157 (2023), 114031.
[23] A.K. Srivastava, A. Banerjee, T. Cui, C. Han, S. Cai, L. Liu, et al., Inhibition of miR-328-3p impairs cancer stem cell function and prevents metastasis in ovarian cancer, Cancer Res. 79 (2019) 2314–2326.
[24] R. Lazova, R.L. Camp, V. Klump, S.F. Siddiqui, R.K. Amaravadi, J.M. Pawelek, Punctate LC3B expression is a common feature of solid tumors and associated with proliferation, metastasis, and poor outcome, Clin. Cancer Res. 18 (2012) 370–379.
[25] C. Han, B. Sun, W. Wang, W. Cai, D. Lou, Y. Sun, et al., Overexpression of microtubule-associated protein-1 light chain 3 is associated with melanoma metastasis and vasculogenic mimicry, Tohoku J. Exp. Med. 223 (2011) 243–251.
[26] Y.-F. Peng, Y.-H. Shi, Z.-B. Ding, A.-W. Ke, C.-Y. Gu, B. Hui, et al., Autophagy inhibition suppresses pulmonary metastasis of HCC in mice via impairing anoikis resistance and colonization of HCC cells, Autophagy 9 (2013) 2056–2068.
[27] S. Galavotti, S. Bartesaghi, D. Faccenda, M. Shaked-Rabi, S. Sanzone, A. McEvoy, et al., The autophagy-associated factors DRAM1 and p62 regulate cell migration and invasion in glioblastoma stem cells, Oncogene 32 (2013) 699.
[28] B. Carroll, N. Mohd-Naim, F. Maximiano, M.A. Frasa, J. McCormack, M. Finelli, et al., The TBC/RabGAP Armus coordinates Rac1 and Rab7 functions during autophagy, Dev. Cell 25 (2013) 15–28.
[29] Y.F. Peng, Y.H. Shi, Z.B. Ding, A.W. Ke, C.Y. Gu, B. Hui, et al., Autophagy inhibition suppresses pulmonary metastasis of HCC in mice via impairing anoikis resistance and colonization of HCC cells, Autophagy 9 (2013) 2056–2068.
[30] M.C. Caino, Y.C. Chae, V. Vaira, S. Ferrero, M. Nosotti, N.M. Martin, et al., Metabolic stress regulates cytoskeletal dynamics and metastasis of cancer cells, J. Clin. Invest. 123 (2013) 2907–2920.
[31] R. Lock, C.M. Kenific, A.M. Leidal, E. Salas, J. Debnath, Autophagy-dependent production of secreted factors facilitates oncogenic RAS-driven invasion, Cancer Discov. 4 (2014) 466–479.
[32] H. Wu, F. Wang, S. Hu, C. Yin, X. Li, S. Zhao, et al., MiR-20a and miR-106b negatively regulate autophagy induced by leucine deprivation via suppression of ULK1 expression in C2C12 myoblasts, Cell. Signal. 24 (2012) 2179–2186.
[33] J.-A. Ju, C.-T. Huang, S.-H. Lan, T.-H. Wang, P.-C. Lin, J.-C. Lee, et al., Characterization of a colorectal cancer migration and autophagy-related microRNA miR-338-5p and its target gene PIK3C3, Biomark. Genom. Med. 5 (2013) 74–78.
[34] R. Lock, C.M. Kenific, A.M. Leidal, E. Salas, J. Debnath, Autophagy-dependent production of secreted factors facilitates oncogenic RAS-driven invasion, Cancer Discov. 4 (2014) 466–479.
[35] S. Comincini, G. Allavena, S. Palumbo, M. Morini, F. Durando, F. Angeletti, et al., microRNA-17 regulates the expression of ATG7 and modulates the autophagy process, improving the sensitivity to temozolomide and low-dose ionizing radiation treatments in human glioblastoma cells, Cancer Biol. Ther. 14 (2013) 574–586.
[36] Y. Chang, W. Yan, X. He, L. Zhang, C. Li, H. Huang, et al., miR-375 inhibits autophagy and reduces viability of hepatocellular carcinoma cells under hypoxic conditions, Gastroenterology 143 (177–87) (2012), e8.
[37] Z. Su, Z. Yang, Y. Xu, Y. Chen, Q. Yu, MicroRNAs in apoptosis, autophagy and necroptosis, Oncotarget 6 (2015) 8474.
[38] M. Deng, H. Tang, Y. Zhou, M. Zhou, W. Xiong, Y. Zheng, et al., miR-216b suppresses tumor growth and invasion by targeting KRAS in nasopharyngeal carcinoma, J. Cell Sci. 124 (2011) 2997–3005.
[39] M.E. Hatley, D.M. Patrick, M.R. Garcia, J.A. Richardson, R. Bassel-Duby, E. Van Rooij, et al., Modulation of K-Ras-dependent lung tumorigenesis by MicroRNA-21, Cancer Cell 18 (2010) 282–293.
[40] R.K. Sahoo, S.K. Tripathi, S. Biswal, M. Panda, S.S. Mathapati, B.K. Biswal, Transforming native exosomes to engineered drug vehicles: a smart solution to modern cancer theranostics, Biotechnol. J. 19 (2024), e2300370.